Preprints of the 19th World Congress
The International Federation of Automatic Control
Cape Town, South Africa. August 24-29, 2014

Performance-Based Sensor Reconfiguration for Fault-Tolerant Control of Uncertain Spatially Distributed Processes

Zhiyuan Yao and Nael H. El-Farra *,1

* *Department of Chemical Engineering & Materials Science University of California, Davis, CA 95616 USA (e-mail: nhelfarra@ucdavis.edu).*

Abstract: This work focuses on the design of a fault detection and fault-tolerant control framework for spatially distributed processes modeled by highly-dissipative partial differential equations (PDEs) subject to external disturbances and sensor faults. The main objective is to devise a suitable sensor reconfiguration strategy to reduce the performance degradation due to the errors resulting from the sensor faults. Initially, a finite-dimensional system that captures the slow dynamics of the PDE is derived and used to design a obverse-based output feedback controller. Using Lyapunov techniques, the fault-free and faulty behavior of the closed-loop system are characterized in terms of the sensor spatial placement, the size of the disturbances, the magnitude of the sensor faults as well as the controller and observer design parameters. Based on the fault-free closed-loop dynamics, the Lyapunov stability bound is used as an alarm threshold to declare the presence of sensor faults. To suppress the performance deterioration, a performance-based sensor reconfiguration policy is developed whereby the supervisor determines either to continue using the current faulty sensors or to switch to suitable backup sensors based on a comparison between the sizes of the achievable terminal sets. A singular perturbation formulation is used to analyze the implementation of the sensor fault-tolerant control structure on the infinite-dimensional system. Finally, the results are illustrated through an application to a representative diffusion-reaction process example.

Keywords: Distributed parameter systems, sensor fault-tolerant control, sensor reconfiguration, transport-reaction processes

1. INTRODUCTION

With the increased complexity of automated industrial control systems, how to achieve a graceful degradation in performance in the presence of faults in the control system components has become a central objective in the control and operation of chemical processes. This is necessitated by the requirements of handling the possible unsatisfactory performance, or even instability, in the event of malfunctions in the sensors, actuators or other system components when applying conventional feedback control designs to a complex system. To overcome these limitations, various approaches to control system design have been developed in order to tolerate component malfunctions while maintaining the desirable stability and performance properties, and hence fault-tolerant control (FTC) has become the focus of considerable research interest over the past few decades in both the academic and industrial circles. Most of the research work in this area, however, has focused on spatially homogeneous processes modeled by systems of ordinary differential equations (e.g., see Simani et al. (2003), Blanke et al. (2003), Steffen (2005), Jiang et al. (2006), Mhaskar et al. (2006), Zhang et al. (2010), Jiang and Yu (2012), Liu et al. (2012) for some results and references), while many systems encountered in the process industry, such as transport-reaction processes, are inherently characterized by the presence of strong spatial variations due to the underlying physical phenomena, such as diffusion, convection and phase dispersion.

While fault-tolerant control of spatially-distributed processes has received increasing attention in recent years (e.g., see Ghantasala and El-Farra (2007), Armaou and Demetriou (2008), Ghantasala and El-Farra (2009), Yao and El-Farra (2011) for some recent results in this area), the majority of efforts in this direction have focused mainly on controller reconfiguration in the event of actuator faults. Sensor faults, on the other hand, have received less attention even thought they are more commonplace in practice and are critical for the overall system performance, especially with the increased reliance on dense sensor deployment and sensor networks in many industrial applications. The measurement errors that can be caused by sensor faults may deteriorate the overall control quality and need to be accounted for explicitly in the control system design and operation.

In this paper, we focus on sensor fault-tolerant control of spatially distributed processes modeled by highly dissipative PDEs under external disturbances. We first develop an observer-based output feedback controller based on a reduced-order model of the PDE to robustly stabilize the closed-loop system in the absence of faults. Using Lyapunov techniques, we investigate the stability proper-

[1] Financial support by NSF, CBET-0747954, is gratefully acknowledged.

ties of the closed loop system for the spatial placement of the measurement sensors and control actuators, and explicitly characterize the terminal regions of the fault-free and faulty closed-loop systems. Based on the fault-free and faulty behaviors of the closed-loop state, a fault detection scheme is developed by monitoring the evolution of the observer state and declaring faults when the state breaches an alarm threshold. A sensor switching strategy is then devised whereby the supervisor can determine to either keep the faulty sensor in use or activate a fall-back sensor configuration based on a comparison of the fault-free and faulty terminal regions.

The rest of the paper is organized as follows. In Section 2, the class of PDEs under consideration is described. Then in Section 3, the observer-based output feedback controller is introduced and the fault detection and performance-based sensor reconfiguration policy are developed for the finite-dimensional closed-loop system. A singular perturbation formulation is then used in Section 4 to derive precise conditions for the implementation of finite-dimensional FD-FTC architecture on the infinite-dimensional system. Finally, the theoretical results are illustrated using a diffusion-reaction process example in Section 5.

2. PRELIMINARIES

As a motivating example, we consider a class of spatially-distributed processes modeled by highly dissipative PDEs of the form:

$$\begin{aligned}\frac{\partial \bar{x}(z,t)}{\partial t} &= \alpha\frac{\partial^2 \bar{x}}{\partial z^2} + \beta\bar{x} + \omega\sum_{i=1}^{m} b_i(z)u_i(t) \\ &\quad + \sum_{j=1}^{p} w_j(\bar{x})d_j(z)\theta_j(t),\ |\theta_j(t)| \le \theta_b^j \end{aligned} \tag{1}$$

$$\begin{aligned} y_l(t) &= \int_0^{\pi} q_l^k(z)\bar{x}(z,t)dz + f_l^k(t), \\ l &\in \{1,\cdots,n\},\ k \in \mathcal{K} \triangleq \{1,\cdots,N\} \end{aligned} \tag{2}$$

subject to the boundary and initial conditions:

$$\bar{x}(0,t) = \bar{x}(\pi,t) = 0,\ \bar{x}(z,t_0) = \bar{x}_0(z) \tag{3}$$

where $\bar{x}(z,t) \in \mathbb{R}$ denotes the process state variable, $z \in [0,\pi]$ is the spatial coordinate, $t \in [t_0,\infty)$ is the time, $u_i \in \mathbb{R}$ denotes the i-th manipulated input, $y(t)$ represents the measured output, m and n are the numbers of manipulated inputs and measured outputs, $b_i(\cdot)$ is the i-th actuator distribution function, $q_l^k(\cdot)$ is the l-th sensor distribution function associated with the k-th sensor configuration, $w_i(\cdot)$ is a sufficiently smooth nonlinear function, $d_j(\cdot)$ is a known function that specifies the positions of action of the bounded uncertain variable θ_j, f_l^k represents a fault in the l-th sensor, $\alpha > 0$ and β are constant parameters, and $\bar{x}_0(z)$ is a smooth function of z. Throughout the paper, the norm notations $|\cdot|$ and $\|\cdot\|$ are used to represent the standard Euclidean norm and the L_2 norm, respectively.

Using standard techniques from operator theory (e.g., see Curtain and Pritchard (1978)), one can represent the PDE of (1)-(3) as an infinite-dimensional system of the form:

$$\dot{x} = \mathcal{A}x + \mathcal{B}u + \mathcal{W}(x)\theta,\ y = \mathcal{Q}x + f^k,\ x(0) = x_0 \tag{4}$$

where $x(t) = \bar{x}(z,t)$, $t > 0$, $z \in [0,\pi]$ is the state function defined on the Hilbert space $\mathcal{H} = L_2(0,\pi)$ endowed with inner product and norm:

$$\langle \omega_1, \omega_2 \rangle = \int_0^{\pi} \omega_1(z)\omega_2(z)dz,\ \|\omega_1\|_2 = \langle \omega_1, \omega_1 \rangle^{\frac{1}{2}} \tag{5}$$

where ω_1, ω_2 are two elements of $L_2(0,\pi)$, $\mathcal{A}$ is the differential operator defined by $\mathcal{A}\phi = \alpha\frac{d^2\phi}{dz^2} + \beta\phi$, $z \in [0,\pi]$, where $\phi(\cdot)$ is a smooth function on $[0,\pi]$ with $\phi(0) = \phi(\pi) = 0$. $\mathcal{B}$ is the input operator defined by $\mathcal{B}u = \omega\sum_{i=1}^{m} b_i(\cdot)u_i$, $\mathcal{W}$ is the uncertainty operator defined by $\mathcal{W}(x)\theta = \sum_{j=1}^{n} w_j(\bar{x})d_j(z)\theta_j(t)$, $x_0 = \bar{x}_0(z)$, $y = [y_1,\cdots,y_n]^T$ and $\mathcal{Q}$ denotes the output operator defined by $\mathcal{Q}x = [\langle q_1, x\rangle,\cdots,\langle q_n, x\rangle]^T$.

By solving the eigenvalue problem $\mathcal{A}\phi_k = \lambda_k\phi_k$, $k \in \{1,\cdots,\infty\}$, the solution can be obtained from $\lambda_k = \beta - \alpha k^2$, $\phi_k(z) = \sqrt{\frac{2}{\pi}}\sin(kz)$, $k \in \{1,\cdot,\infty\}$, where λ_k and ϕ_k denote the k-th eigenvalue and eigenfunction, respectively. By analyzing this solution, it can be seen that all the eigenvalues of $\mathcal{A}$ are real and ordered. Also, for a given α only a finite number of unstable eigenvalues exists, and the distance between two consecutive eigenvalues (i.e., λ_k and λ_{k+1}) increases as k increases. Furthermore, the spectrum of A can be partitioned as $\sigma(\mathcal{A}) = \sigma_1(\mathcal{A}) \cup \sigma_2(\mathcal{A})$; where $\sigma_1(\mathcal{A}) = \{\lambda_1,\cdots,\lambda_m\}$ contains the first m (with m finite) "slow" eigenvalues and $\sigma_2(\mathcal{A}) = \{\lambda_{m+1},\lambda_{m+2},\cdots\}$ contains the remaining "fast" stable eigenvalues where $|\lambda_m|/|\lambda_{m+1}| = O(\epsilon)$ and $\epsilon < 1$ is a small positive number that characterizes the extent of separation between the slow and fast eigenvalues of $\mathcal{A}$. This separation property implies that the dominant dynamics of the PDE can be described by a finite-dimensional system, and motivates the application of modal decomposition techniques to decompose the infinite-dimensional system of (4) into the following interconnected subsystems (see Christofides and Daoutidis (1996), Christofides (2001)):

$$\dot{x}_s = \mathcal{A}_s x + \mathcal{B}_s u + \mathcal{W}_s(x_s,x_f)\theta,\ x_s(0) = \mathcal{P}_s x_0 \tag{6}$$

$$\dot{x}_f = \mathcal{A}_f x + \mathcal{B}_f u + \mathcal{W}_f(x_s,x_f)\theta,\ x_f(0) = \mathcal{P}_f x_0 \tag{7}$$

$$y = \mathcal{Q}_s x_s + \mathcal{Q}_f x_f + f^k \tag{8}$$

where $x_s = \mathcal{P}_s x \in \mathcal{H}_s := \text{span}\{\phi_1,\cdots,\phi_m\}$ is the state of a finite dimensional system that describes the evolution of the slow modes, $x_f = \mathcal{P}_f x \in \mathcal{H}_f := \text{span}\{\phi_{m+1},\phi_{m+2},\cdots\}$ is the state of an infinite dimensional system that captures the evolution of the fast eigenvalues, $\mathcal{H}_s$, $\mathcal{H}_f$ are modal subspaces of $\mathcal{A}$, and $\mathcal{P}_s$ and $\mathcal{P}_f$ are the orthogonal projection operators, where $\mathcal{A}_s = \mathcal{P}_s\mathcal{A}$ is an $m \times m$ diagonal matrix of the form $\mathcal{A} = \text{diag}\{\lambda_1,\cdots,\lambda_m\}$, $\mathcal{B}_s = \mathcal{P}_s\mathcal{B}$, $\mathcal{W}_s = \mathcal{P}_s\mathcal{W}$ and $\mathcal{Q}_s = \mathcal{P}_s\mathcal{Q}$. $\mathcal{A}_f = \mathcal{P}_f\mathcal{A}$ is an unbounded differential operator which is exponential stable (following from the fact that $\lambda_{m+1} < 0$ and the selection of $\mathcal{H}_s$ and $\mathcal{H}_f$), $\mathcal{B}_f = \mathcal{P}_f\mathcal{B}$, $\mathcal{W}_f = \mathcal{P}_f\mathcal{W}$ and $\mathcal{Q}_f = \mathcal{P}_f\mathcal{Q}$. In what follows, the x_s- and x_f-subsystems will be referred to as the slow and fast subsystems, respectively. Neglecting the fast and stable x_f-subsystem of (7), the following approximate, m-dimensional slow system can be obtained:

$$\dot{\bar{x}}_s = \mathcal{A}_s x + \mathcal{B}_s u + \mathcal{W}_s(\bar{x}_s,0)\theta,\ y = \mathcal{Q}_s x_s + f^k \tag{9}$$

where the bar symbol denotes that the variable is associated with a finite-dimensional system.

3. FINITE-DIMENSIONAL SENSOR FAULT-TOLERANT CONTROL

3.1 Output feedback controller synthesis

The focus of this section is on the design of the proposed sensor fault-tolerant control structure. Due to the lack

of full state measurement, we first introduce a finite-dimensional state observer to estimate the evolution of the slow state and use it to synthesize an observer-based output feedback controller of the form:

$$u^k = \mathcal{F}^k\eta,\ \dot{\eta} = \widehat{\mathcal{A}}_s\eta + \widehat{\mathcal{B}}_s u^k + \mathcal{L}^k(\bar{y} - \mathcal{Q}_s^k\eta) \tag{10}$$

where η is an observer estimate of $\bar{x}_s$, $\widehat{\mathcal{A}}_s$ and $\widehat{\mathcal{B}}_s$ are bounded operators that represent models of $\mathcal{A}_s$ and $\mathcal{B}_s$, respectively, $\mathcal{F}^k$ and $\mathcal{L}^k$ are the controller and observer gains associated with the k-th configuration.

Considering the output feedback controller of (10) is implemented on the fault-free slow system of (9) (i.e., with $f^k = 0$) and defining the augmented state as $\bar{\xi} = [\bar{x}_s,\ \eta]^T$, which is an element of the extended state space $\mathcal{H}_s^{\xi} \triangleq \mathcal{H}_s \times \mathcal{H}_s$, the closed-loop system can be expressed in the following augmented formulation:

$$\dot{\bar{\xi}} = \Lambda^k\bar{\xi} + \Gamma\theta,\ \|\,\theta(t)\,\| \le \theta_b \tag{11}$$

where

$$\Lambda^k = \begin{bmatrix} \mathcal{A}_s & \mathcal{B}_s\mathcal{F}^k \\ \mathcal{L}^k\mathcal{Q}_s^k & \widehat{\mathcal{A}}_s + \widehat{\mathcal{B}}_s\mathcal{F}^k - \mathcal{L}^k\mathcal{Q}_s^k \end{bmatrix},\ \Gamma = \begin{bmatrix} \mathcal{W}_s \\ \mathcal{O} \end{bmatrix}$$

Examining the structure of the above augmented system, it can be seen that by proper selection of $\mathcal{F}^k$ and $\mathcal{L}^k$ one can ensure exponential stability of the origin of the unperturbed closed-loop system of (11) (i.e., with $\theta = 0$). From converse Lyapunov theorems, there exists a continuously differentiable function $V(\bar{\xi})$ defined by $V(\bar{\xi}) = \bar{\xi}^T P^k \bar{\xi}$ such that $(\Lambda^k)^T P^k + P^k\Lambda^k = -Q$ holds, where $P^k,\ Q$ are real symmetric positive-definite matrices. Then, by analyzing the evolution of $V(\bar{\xi})$ along the trajectories of the closed-loop augmented system of (11), the following inequality can be obtained:

$$\dot{V}(\bar{\xi}) \le -\lambda_{\min}(Q)\|\,\bar{\xi}\,\|^2 + 2\|\,\bar{\xi}\,\|\|\,P^k\Gamma\,\|\theta_b$$

and it can be shown that $\dot{V}(\bar{\xi}) < 0$, if

$$\|\,\bar{\xi}\,\| > \bar{\gamma}_1^k(z_s^k, \theta_b) \triangleq 2\lambda_{\min}^{-1}(Q)\|\,P^k\Gamma\,\|\theta_b$$

This result indicates that practical stability of the augmented closed-loop system of (11) is achieved, leading to the existence of a terminal region associated with fault-free closed-loop system of (11) and defined by:

$$\bar{\mathcal{T}}^k(z_s^k, \theta_b) \triangleq \{\bar{\xi} : \|\,\bar{\xi}\,\| \le \bar{\gamma}_1^k(z_s^k, \theta_b)\} \tag{12}$$

Remark 1. The existence of a fault-free terminal region, $\bar{\mathcal{T}}^k(z_s^k, \theta_b)$, implies that the trajectories of the closed-loop system of (11) converge to $\bar{\mathcal{T}}^k(z_s^k, \theta_b)$ in finite time and never leave. From the definition of $\bar{\mathcal{T}}^k(z_s^k, \theta_b)$, it can be observed that the size of the terminal region is dependent on the spatial placement of the sensors, z_s^k, the size of the disturbances, θ_b, and the controller and observer design parameters, ($\mathcal{F}^k$, $\mathcal{L}^k$). Therefore, the performance of the closed-loop system is influenced by how these various design parameters are chosen. Specifically, even though a large disturbance may result in a large terminal region (and thus poor performance), one may be able to improve the closed-loop performance by placing the sensors and actuators at locations which are more robust to the external disturbance (i.e., the locations with smaller terminal regions).

Based on the fault-free behavior of the augmented system of (11), we can then analyze the evolution of the closed-loop state when faults take place in some of the active sensors (i.e., $f^k \neq 0$). We consider the case when these faults can be properly detected and satisfy some measurable bound. The augmented system in the presence of sensor faults can then be formulated as follows:

$$\dot{\bar{\xi}} = \Lambda^k\bar{\xi} + \Gamma\theta + \Pi^k f^k,\ \|\,\theta(t)\,\| \le \theta_b,\ \|\,f^k(t)\,\| \le f_b^k \tag{13}$$

where Π^k is an operator matrix defined by $\Pi^k = [\mathcal{O},\ \mathcal{L}^k]^T$. Following the same analysis approach used for the fault-free augmented system, it can be verified that the time-derivative of $V(\bar{\xi})$ along the trajectories of the closed-loop system of (13) satisfies the following inequality:

$$\dot{V}(\bar{\xi}) \le -\lambda_{\min}(Q)\|\,\bar{\xi}\,\|^2 + 2\|\,\bar{\xi}\,\|(\|\,P^k\Gamma\,\|\theta_b + \|\,P^k\Pi\,\|f_b^k)$$

Comparing this inequality with the one obtained for the fault-free system, it can be seen that the bound on $\dot{V}(\bar{\xi})$ increases due to the effect of sensor faults. As a result, the decaying trend of $V(\bar{\xi})$ can be maintained ($\dot{V}(\bar{\xi}) < 0$), only when

$$\|\,\bar{\xi}\,\| > \bar{\gamma}_2^k(z_s^k, \theta_b, f_b^k) \triangleq 2\lambda_{\min}^{-1}(Q)(\|\,P^k\Gamma\,\|\theta_b + \|\,P^k\Pi\,\|f_b^k)$$

and, therefore, the terminal region in the presence of sensor faults is also enlarged as:

$$\bar{\mathcal{S}}^k(z_s^k, \theta_b, f_b^k) \triangleq \{\bar{\xi} : \|\,\bar{\xi}\,\| \le \bar{\gamma}_2^k(z_s^k, \theta_b, f_b^k)\}. \tag{14}$$

Remark 2. Note from the definitions of $\bar{\mathcal{T}}^k(z_s^k, \theta_b)$ and $\bar{\mathcal{S}}^k(z_s^k, \theta_b, f_b^k)$ that the ultimate bound derived for the faulty system is additionally parameterized by the magnitude of the sensor faults. This is consistent with the intuition that the deterioration of the closed-loop performance becomes more significant in the presence of more severe sensor faults. In addition, as can be seen from (12) and (14), the fault-free and faulty terminal regions exhibit similar dependencies on the sensor locations, z_s^k, such that sensor configurations with larger $\bar{\mathcal{T}}^k(z_s^k, \theta_b)$ have larger $\bar{\mathcal{S}}^k(z_s^k, \theta_b, f_b^k)$ as well.

3.2 Sensor fault detection scheme

The closed-loop behaviors obtained fore the fault-free and faulty augmented systems provide a way to derive some rules for sensor fault detection in the finite-dimensional closed-loop system. The key idea is to monitor the evolution of the state and use the fault-free ultimate bound $\bar{\gamma}_1^k(z_s^k, \theta_b)$ as an alarm threshold to declare a fault in the operating sensor configuration. As can be seen from the definition of the fault-free terminal region $\bar{\mathcal{T}}^k(z_s^k, \theta_b)$, the implementation of the above fault detection scheme requires the state measurement $\bar{x}_s$, which in practice is not available. To deal with this limitation, the evolution of the observer state, η, is monitored instead, and we define a new monitoring set in terms of η which can be expressed as:

$$\widehat{\mathcal{T}}^k(z_s^k, \theta_b) \triangleq \{\eta : \|\,\eta(t)\,\| \le \bar{\gamma}_1^k(z_s^k, \theta_b)\} \tag{15}$$

Since η is a component of the augmented state, $\bar{\xi}$, the detection of η outside the terminal set $\widehat{\mathcal{T}}^k(z_s^k, \theta_b)$ always indicates the fact that $\bar{\xi}$ has already breached $\bar{\mathcal{T}}^k(z_s^k, \theta_b)$. Applying the new monitoring set $\widehat{\mathcal{T}}^k(z_s^k, \theta_b)$ to the proposed fault detection logic, a fault can be declared at time $T_d > T_c$ if η breaches the alarm threshold $\bar{\gamma}_1^k(z_s^k, \theta_b)$, i.e.,:

$$\|\,\eta(T_d)\,\| > \bar{\gamma}_1^k(z_s^k, \theta_b) \Rightarrow f^k(T_d) \neq 0 \tag{16}$$

where T_d is the time when the faults are detected, T_c is the earliest time when η converges into $\widehat{\mathcal{T}}^k(z_s^k, \theta_b)$ defined as $T_c \triangleq \min\{t : \|\,\eta(t)\,\| \le \bar{\gamma}_1^k(z_s^k, \theta_b)\}$. Applying a similar approach to the faulty system of (13), a new monitoring set for the observer estimate η can be obtained as follows:

$$\widehat{\mathcal{S}}^k(z_s^k, \theta_b, f_b^k) \triangleq \{\eta : \|\,\eta(t)\,\| \le \bar{\gamma}_2^k(z_s^k, \theta_b, f_b^k)\} \tag{17}$$

Note that having η escape from $\widehat{\mathcal{S}}^k(z_s^k, \theta_b, f_b^k)$ at some time is an indication that the augmented state, $\bar{\xi}$, has already moved out of $\bar{\mathcal{S}}^k(z_s^k, \theta_b, f_b^k)$.

Remark 3. It should be noted that the alarm threshold, $\bar{\gamma}_1^k(z_s^k, \theta_b)$, accounts for the influences of the external disturbances and is used to declare a fault after the process state has already converged into the fault-free terminal region. For the case when $t < T_c$ (i.e., prior ro convergence to the terminal set), a time-varying alarm threshold can be applied based on the analysis of fault-free dynamics of η. Moreover, the presence of a sensor fault cannot be detected immediately but requires a short period time until η breaches $\widehat{\mathcal{T}}^k(z_s^k, \theta_b)$. This detection delay can be minimized by proper choices of the sensor/actuator locations as well as the controller and observer design parameters ($\mathcal{F}^k$,$\mathcal{L}^k$) to ensure that the threshold is sufficiently tight.

3.3 Performance-based sensor reconfiguration policy

Following the declaration of a fault in the operating sensor configuration, we need to determine whether a corrective action in the form of switching to a healthy fall-back sensor configuration needs to be executed based on the knowledge of the sensor fault. From the dependence of the terminal regions, $\bar{\mathcal{T}}^k(z_s^k, \theta_b)$ and $\bar{\mathcal{S}}^k(z_s^k, \theta_b, f_b^k)$, on sensor locations z_s^k, it can be verified that keeping the faulty sensor configuration active (subject to a non-critical fault) may provide better closed-loop performance than activating a fall-back sensor configuration in cases where the faulty terminal region, $\bar{\mathcal{S}}^i(z_s^i, \theta_b, f_b^i)$, is smaller than the fault-free terminal region subject to the backup configuration, $\bar{\mathcal{T}}^j(z_s^j, \theta_b)$. In that case, the faulty sensor configuration should be kept in use, even after the existing sensor fault has been detected. On the other hand, when $\bar{\mathcal{S}}^i(z_s^i, \theta_b, f_b^i)$ becomes larger than $\bar{\mathcal{T}}^j(z_s^j, \theta_b)$ due to a severe fault taking place, the backup sensor configuration corresponding to the smallest fault-free terminal region among all the feasible configurations must be activated to replace the faulty sensor configuration. This logic is formalized in Theorem 1 below. The proof is conceptually straightforward and is omitted for brevity.

Theorem 1. Consider the closed-loop system of (13), where $\| \theta(t) \| \leq \theta_b$ and $\| f^k(t) \| \leq f_b^k$, for some θ_b, $f_b^k > 0$. Let $T_f^{i_k}$ be the earliest time such that the i_k-th fault is detected. Then the following switching rule:

$$k(t) = \begin{cases} i_0 = \arg\min_{i \in \mathcal{K}} \bar{\gamma}_1^i, & \forall\ t \in [t_0, t_1) \\ i_1 = \arg\min_{i \in \mathcal{K}, i \neq i_0} \{\bar{\gamma}_1^i, \bar{\gamma}_2^{i_0}\}, & \forall\ t \in [t_1, t_2) \\ \vdots & \vdots \\ i_j = \arg\min_{i \in \mathcal{K}, i \neq i_{j-1}} \{\bar{\gamma}_1^i, \bar{\gamma}_2^{i_{j-1}}\}, & \forall\ t \in [t_j, t_{j+1}) \end{cases} \tag{18}$$

guarantees that the state of the closed-loop system is ultimately bounded.

4. SENSOR FAULT-TOLERANT CONTROL OF THE INFINITE-DIMENSIONAL SYSTEM

4.1 Fault-free controller implementation

Considering the design of fault-tolerant control structure described in the previous section is implemented using the measured outputs of the infinite-dimensional system of (6)-(8), the observer-based output feedback controller can be formulated as follows:

$$u^k = \mathcal{F}^k \eta,\ \dot{\eta} = \widehat{\mathcal{A}}_s \eta + \widehat{\mathcal{B}}_s u^k + \mathcal{L}^k (y - \mathcal{Q}_s^k \eta) \tag{19}$$

which has a similar structure to the controller of (10), except that the output y (instead of $\bar{y}$) is used to implement the observer. Introducing the augmented state $\xi = [x_s,\ \eta]^T$, we can express the infinite-dimensional augmented system in the following singularly perturbed form (see Christofides (2001) for the basis and details of this formulation):

$$\dot{\xi} = \Lambda^k \xi + \Theta\theta + \Xi x_f + \Pi^k f^k \tag{20}$$

where $\Theta \triangleq [\mathcal{W}_s(x_s, x_f),\ \mathcal{O}]^T$ (with $\Theta = \Gamma$ when $x_f = 0$), and $\Xi \triangleq [\mathcal{O},\ \mathcal{L}^k \mathcal{Q}_f]^T$. Note that the slow and fast subsystems are coupled together due to the use of the output of the infinite-dimensional system which contains both the slow and fast states. The stability properties of the infinite-dimensional closed-loop system are summarized in the following proposition, which ties the controller design with the separation between the slow and fast eigenvalue of $\mathcal{A}$. The result can be justified using singular perturbation techniques.

Proposition 2. Consider the infinite-dimensional system of (6)-(8), with $f^k(t) \equiv 0$ for a fixed $k \in \mathcal{K}$, subject to the control law of (19) and choose $\mathcal{F}^k$ and $\mathcal{L}^k$ such that Λ^k is exponentially stable. Then exists a positive real number, ϵ^*, such that if $\epsilon \in [0, \epsilon^*)$, the zero solution of the infinite-dimensional closed-loop system is stable and the closed-loop state is ultimately bounded.

Remark 4. According to the result of Proposition 2, the output feedback controller that stabilizes the approximate finite-dimensional system continues to stabilize the infinite-dimensional system provided that the separation between the slow and fast eigenvalues is sufficiently large. This restriction, which requires that a sufficient number of slow states be included in the finite-dimensional controller design, is needed to ensure that the error introduced by using y instead of $\bar{y}$ is sufficiently small.

4.2 Sensor fault detection and reconfiguration

In the controller implementation on the infinite-dimensional system, the observer estimates are generated using y (which depends on both x_s and x_f) instead of $\bar{y}$ which was used in the finite-dimensional case. Consequently, some modifications must be made to the fault-free and faulty terminal regions to minimize the false alarms which could result from the approximation error made in neglecting x_f when deriving the approximate finite-dimensional system. These modifications are summarized in the following proposition and can be used as an alarm threshold to decide conclusively when a fault can be declared and consequently when to switch sensor configurations in the infinite-dimensional system. The proof is omitted for brevity.

Proposition 3. Consider the infinite-dimensional system of (6)-(8), subject to the control law of (19) where $\mathcal{F}^k$ and $\mathcal{L}^k$ are chosen such that Λ^k is exponentially stable. Then given any set of positive real numbers $\{d, T_1, T_b < T_1\}$, there exists a positive real number $\widehat{\epsilon}$ such that the fault-free and faulty threshold $\gamma_1^k(z_s^k, \theta_b)$ and $\gamma_2^k(z_s^k, \theta_b, f_b^k)$ of the observer estimate η satisfy, $\forall\ t \in [T_b, T_1]$,

$$\gamma_1^k(z_s^k, \theta_b) = \bar{\gamma}_1^k(z_s^k, \theta_b) + d \tag{21}$$

$$\gamma_2^k(z_s^k, \theta_b, f_b^k) = \bar{\gamma}_2^k(z_s^k, \theta_b, f_b^k) + d \tag{22}$$

Remark 5. Proposition 3 introduces three modifications to the fault detection and fault reconfiguration scheme developed based on the approximate finite-dimensional system. The first modification involves enlarging the fault detection alarm threshold by $d = O(\epsilon)$, which reflects the size of the approximation error. Notice, however, that d can be chosen arbitrarily small provided that ϵ is sufficiently small. The second modification is evaluating the residual only after a small period of time $[0, T_b]$ has elapsed to ensure that x_f has converged sufficiently close to zero. This waiting period can also be made small if ϵ is sufficiently small. The final modification is limiting the time window for fault detection to a finite time-interval $[T_b, T_1]$. The reason for this is the fact that, owing to the bounded stability of the fault-free closed-loop system, closeness between the solution of the finite-dimensional and infinite-dimensional systems can be established only over a finite time interval. This fault detection window, however, can be made as large as desired provided that ϵ is sufficiently small.

Remark 6. Similar to the way that the output feedback control and fault detection strategies are implemented, one can show using singular perturbation arguments that the sensor reconfiguration logic of (18) which is based on the approximate finite-dimensional system continues to enforce closed-loop stability in the infinite-dimensional system and to guarantee the best control performance among all the possible fall-back choices provided that ϵ is sufficiently small.

5. SIMULATION STUDY: APPLICATION TO A DIFFUSION-REACTION PROCESS

We consider the following representative diffusion-reaction process which describes a long, thin catalytic rod in a reactor with a zeroth-order exothermic reaction taking place on the rod. Under standard modeling assumptions, the spatiotemporal evolution of the dimensionless rod temperature is described by:

$$\begin{aligned} \frac{\partial \bar{x}}{\partial t} &= \frac{\partial^2 \bar{x}}{\partial z^2} + (\beta_T \gamma e^{-\gamma} - \beta_U)\bar{x} + \beta_U b(z) u + d(z)\theta \\ y_l &= \int_0^\pi q_l(z)\bar{x} dz + f_l(t),\ l = 1, \cdots, n \end{aligned} \tag{23}$$

subject to boundary conditions $\bar{x}(0,t) = \bar{x}(\pi,t) = 0$, where $\bar{x}$ denotes the dimensionless temperature, $\beta_T = 50.0$, $\gamma = 2.0$, $\beta_U = 4.0$ denote dimensionless heat of reaction, activation energy and heat transfer coefficient, respectively, $u(t)$ denotes the dimensionless temperature of the cooling medium, θ is a parametric uncertainty in the heat of reaction, and $b(z)$ is the actuator distribution function. It can be verified that the operating steady state $\bar{x}(z,t) = 0$ (with $u = \theta = 0$) is unstable. The control objective is to stabilize the temperature profile near this unstable, spatially uniform steady state by manipulating the temperature of the cooling medium, in the presence of uncertainty and sensor faults.

The solution of the eigenvalue problem for the differential operator yields $\lambda_j = \beta_T \gamma e^{-\gamma} - \beta_U - j^2$, $\phi_j(z) = \sqrt{\frac{2}{\pi}} \sin(jz)$, $j \in \{1, 2, \cdots, \infty\}$. The first eigenmode is chosen as the dominant one since only the first eigenvalue

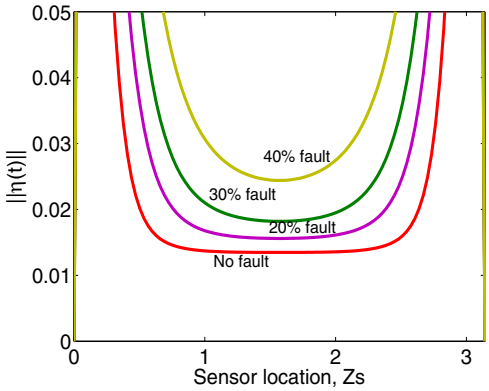

Fig. 1. Dependence of fault-free and faulty terminal regions on the sensor spatial placement.

is positive, and Galerkins method is applied to derive an ODE that describes the approximate temporal evolution of the amplitude of the first eigenmode:

$$\dot{\bar{a}}_1 = \lambda_1 \bar{a}_1 + g(z_a)u + w(z)\theta_1 \tag{24}$$

where $\bar{x}(z,t) = \sum_{i=1}^{\infty} a_i(t)\phi_i(z)$, $g(z_a) = \beta_U \langle \phi_1(z), b(z) \rangle$, $w(z) = \beta_U \langle \phi_1(z), d(z) \rangle$, and a single point actuator (with finite support) at $z_a = 0.5\pi$ is used for stabilization, i.e., $b(z) = 1/(2\mu)$ for $z \in [z_a - \mu, z_a + \mu]$, where μ is a sufficiently small positive number and $b(z) = 0$ elsewhere. Similarly, a point sensor is also used to measure the output of the process, and a point heat source is introduced at 0.5π as an external disturbance with $\theta_b = 0.02$. The above ODE is used to design the sensor fault detection and reconfiguration scheme which is then implemented on a 30-th order Galerkin discretization of the PDE (higher-order discretizations gave the same results).

In Fig.1, the size of the fault-free terminal region and the terminal regions subject to sensor faults with different magnitudes are compared, for different placement of the measurement sensor. As can be observed, the fault-free and faulty terminal regions exhibit the same dependency on the sensor location, and the terminal region is enlarged as the severity level of the sensor fault increases. Moreover, it can be seen that all the terminal regions shrink as the sensor is moved closer to the middle of the spatial domain which implies better closed-loop performance.

In order to demonstrate how the developed FD-FTC scheme is implemented, we first consider the case when the operating sensor is placed at $z_s = 1.5$ with 2 backup sensors at 0.7π and 0.8π. From Fig.2(a), it can be seen that when a 40% fault (sensor measurement is 60% of the actual output measurement) takes place at $t = 3.5$, it cannot be detected immediately but need to wait a short period of time until $t = 4.8$ when η breaches the alarm threshold. Then, we need to determine whether to switch to one of the backup sensors or to keep using the current faulty sensor. Comparing the terminal region subject to 40% fault with $z_s = 1.5$ and the fault-free terminal region with $z_s = 0.7\pi$ and $z_s = 0.8\pi$ in Fig.2(b), it can be seen that both backup configurations can reduce the degradation of the closed-loop performance, while switching to $z_s = 0.7\pi$ is the best choice because its leads to a smaller terminal region than the one for $z_s = 0.8\pi$. This prediction can be confirmed by the comparison of the observer state, the amplitude of the first eigenmode, and the control action profiles depicted in

Figs.2(a), (c) and (d). As expected, the choice of using the current faulty sensor leads to the worst performance, while the smallest offset is achieved by switching to the backup sensor at $z_s = 0.7\pi$.

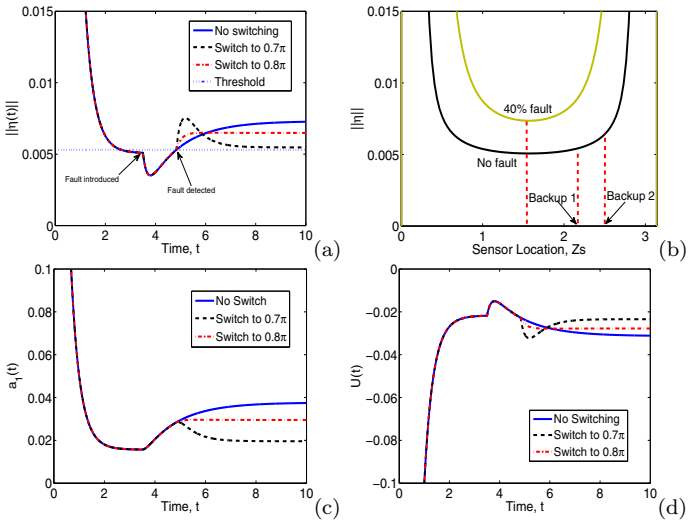

Fig. 2. Plot (a): Observer state profiles when a 40% fault is introduced at $t = 3.5$. Plot (b): Terminal region profiles for different sensor configurations. Plots (c)-(d): The amplitude of the first eigenmode and the control action profiles for different sensor configurations.

When a sensor fault is detected, switching to a backup sensor may not always result in an improvement in the closed-loop performance. In order to demonstrate this possibility, we consider another scenario where the backup sensor is placed at $z_s = 0.95\pi$, near the boundary of the process and a 30% fault takes place at $t = 3.5$. From the terminal region profile in Fig.3(a), it can be observed that the fault-free terminal set for the backup sensor is larger than the current faulty terminal region. Therefore, no sensor switching is required after detection of the sensor fault. This prediction is then confirmed by the comparison of the observer state and the closed-loop state profiles in Figs.3 (b)-(d), where the offset of the closed-loop state for $z_s = 0.5\pi$ is much smaller than the one for the backup configuration at $z_s = 0.95\pi$.

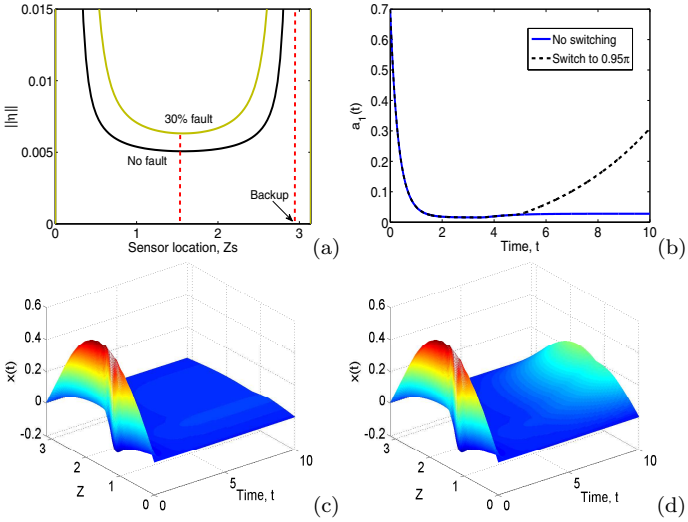

Fig. 3. Plot (a): Terminal region profiles for different sensor configurations. Plots (b)-(d): The amplitude of the first eigenmode and the closed-loop state profiles for the case when no switching is performed and for the case of switching to a backup sensor at $z_s = 0.95\pi$, when a 30% fault takes place at $t = 3.5$.

REFERENCES

Armaou, A. and Demetriou, M. (2008). Robust detection and accommodation of incipient component faults in nonlinear distributed processes,. *AIChE J.*, 54, 2651–2662.

Blanke, M., Kinnaert, M., Lunze, J., and Staroswiecki, M. (2003). *Diagnosis and Fault-Tolerant Control*. Springer, Berlin-Heidelberg.

Christofides, P.D. (2001). *Nonlinear and Robust Control of PDE Systems: Methods and Applications to Transport-Reaction Processes*. Birkhäuser, Boston.

Christofides, P.D. and Daoutidis, P. (1996). Nonlinear control of diffusion-convection-reaction processes. *Comp. & Chem. Eng.*, 20, 1071–1076.

Curtain, R.F. and Pritchard, A.J. (1978). *Infinite Dimensional Linear Systems Theory*. Springer-Verlag, Berlin-Heidelberg.

Ghantasala, S. and El-Farra, N.H. (2007). Robust fault detection and handling in uncertain transport-reaction processes. *Dynam. Contin. Dis. & Impul. Syst. (Series A)*, 14, 203–208.

Ghantasala, S. and El-Farra, N.H. (2009). Robust actuator fault isolation and management in constrained uncertain parabolic pde systems. *Automatica*, 45, 2368–2373.

Jiang, B., Staroswiecki, M., and Cocquempot, V. (2006). Fault accommodation for nonlinear dynamic systems. *IEEE Trans. Automat. Contr.*, 51, 1578–1583.

Jiang, J. and Yu, X. (2012). Fault-tolerant control systems: A comparative study between active and passive approaches. *Annu. Rev. in Contr.*, 36, 60–72.

Liu, L., Shen, Y. Dowell, E.H., and Zhu, C. (2012). A general fault tolerant control and management for a linear system with actuator faults. *Automatica*, 48, 1676–1682.

Mhaskar, P., Gani, A., and Christofides, P.D. (2006). Fault-tolerant control of nonlinear processes:performance-based reconfiguration and robustness. *Int. J. Robust Nonlin. Contr.*, 16, 91–111.

Simani, S., Fantuzzi, C., and Patton, R. (2003). *Model-based Fault Diagnosis in Dynamic Systems Using Identification Techniques*. Springer, London.

Steffen, T. (2005). *Control reconfiguration of dynamic systems: Linear approaches and structural tests*. Springer, Berlin, Germany.

Yao, Z. and El-Farra, N.H. (2011). Robust fault detection and reconfigurable control of uncertain sampled-data distributed processes. In *Proceedings of 50th IEEE Conference on Decision and Control*, 4925–4930. Orlando, FL.

Zhang, X., Polycarpou, M.M., and Parisini, T. (2010). Fault diagnosis of a class of nonlinear uncertain systems with lipschitz nonlinearities using adaptive estimation. *Automatica*, 46, 290–299.